



Carbon nanotube array as a van der Waals two-dimensional hyperbolic material

R. G. Polozkov * and N. Y. Senkevich
ITMO University, Saint Petersburg 197101, Russia

S. Morina
Science Institute, University of Iceland, Dunhagi 3, IS-107 Reykjavik, Iceland

P. Kuzhir 
Institute of Photonics, University of Eastern Finland, Yliopistokatu 7, FI-80101 Joensuu, Finland
and Belarusian State University, Institute for Nuclear Problems, Minsk 220006 Bobruiskaya 11, Belarus

M. E. Portnoi 
ITMO University, Saint Petersburg 197101, Russia;
School of Physics, University of Exeter, Stocker Road, Exeter EX4 4QL, United Kingdom;
and International Institute of Physics, Universidade Federal do Rio Grande do Norte, Natal-RN 59078-970, Brazil

I. A. Shelykh
ITMO University, Saint Petersburg 197101, Russia
and Science Institute, University of Iceland, Dunhagi 3, IS-107 Reykjavik, Iceland



(Received 16 April 2019; revised manuscript received 17 October 2019; published 2 December 2019)

We use an *ab initio* approach to design and study a two-dimensional material—a planar array of carbon nanotubes separated by an optimal distance defined by the van der Waals interaction. We show that the energy spectrum for an array of quasimetallic nanotubes is described by a strongly anisotropic hyperbolic dispersion and formulate a model low-energy Hamiltonian for its semianalytical treatment. Periodic-potential-induced lifting of the valley degeneracy for an array of zigzag narrow-gap nanotubes leads to the band-gap collapse. In contrast, the band gap is opened in an array of gapless armchair tubes. These unusual spectra, marked by pronounced van Hove singularities in the low-energy density of states, open the opportunity for interesting physical effects and prospective optoelectronic applications.

DOI: [10.1103/PhysRevB.100.235401](https://doi.org/10.1103/PhysRevB.100.235401)

I. INTRODUCTION

One of the recent trends in contemporary nanotechnology is the use of van der Waals heterostructures for band-structure engineering [1,2]. This trend closely followed the seminal work on exfoliation of graphene with its unique electronic properties, which also provided a major boost to carbon-based optoelectronics. Exfoliation of graphene was in turn preceded by over a decade of extensive study of carbon nanotubes, following the pioneering work of Iijima [3], which still dwarfs any other publication on carbon-based nanostructures in the number of citations. In this paper, we attempt to marry the van der Waals heterostructures' band-structure engineering with the rich physics of carbon nanotubes in an attempt to design a self-organized metamaterial with hyperbolic dispersion.

Carbon nanotubes (CNTs) have been studied extensively since their discovery [3]. The search for new applications based on their unique mechanical and electronic properties is intensifying. In particular, the high and gate-tunable electrical

conductivity of CNT-based quantum wires provides a potential solution for on-chip interconnects and transistors in future integrated circuits [4]. Depending on the community-specific interests and targeted applications, nanotubes are considered as either single molecules or quasi-one-dimensional crystals with translational periodicity [5].

The electronic properties of single-walled CNTs are fully determined by the way they are rolled from a graphene sheet, as described in detail in the vast number of papers, reviews, and textbooks. In what follows, we use the most common notations for CNT rolling adopted from Refs. [6,7].

Recently, significant progress has been achieved in the controlled growth of horizontally aligned carbon nanotube (HACN) arrays [8–12]. Such structures show great potential as building blocks for transparent displays, nanoelectronics, quantum communication lines, field-emission transistors, superstrong tethers, and aeronautics and astronautics materials. CNT optical properties have been utilized in highly efficient HACN-based terahertz (THz) polarizers [13,14] and optically excited THz emitters [15–17]. Other notable features of HACN arrays include giant midinfrared intersubband transitions [18] and recently predicted exciton ground-state

*polozkov@itmo.ru

brightening [19] in the polarization-sensitive strong-coupling regime [20].

The optical properties of planar HACN arrays have been a subject of extensive research, whereas the in-plane electronic transport, which should be highly anisotropic, has not been extensively studied. In particular, it would be interesting to look at the low-energy electronic spectrum of an array of metallic nanotubes. Indeed, graphene with its linear quasi-particle energy spectrum has become a popular “playground” to study ultrarelativistic phenomena on the tabletop. It could be expected that aligning metallic single-walled carbon nanotubes in a regular array may produce an even more interesting dispersion. In this respect, zigzag ($3p, 0$) CNTs should be more promising than armchair tubes. Indeed, ($3p, 0$) nanotubes are, in fact, quasimetallic with tiny curvature-induced gaps [21], which are highly sensitive to the environment. In addition, the energy-spectrum degeneracy near the “double” Dirac point in zigzag CNTs, which stems from the graphene valley degeneracy and the way these nanotubes are rolled, promises a significantly richer in-plane dispersion in a regular array in comparison to the case of armchair nanotubes, in which the two Dirac points are well separated in momentum space. For armchair CNTs, the main effect of introducing periodicity in the direction normal to the nanotube axis should be the opening of a small band gap, whereas degeneracy lifting in zigzag tubes is expected to result in a very complex dispersion stemming from crossings and avoided crossings of various energy levels. Therefore, our study will be mostly focused on narrow-gap zigzag CNTs, with only limited results for armchair tubes of similar diameter presented mostly for comparison. Our approach to this problem is based on *ab initio* calculations, which allows us to simultaneously find the optimal distance between nanotubes in the array which minimizes the total energy and the in-plane energy spectrum. *Ab initio* methods are widely used to study electronic properties of single carbon nanotubes with different chiralities [22,23] and various complex systems based on carbon nanotubes [5,24]. On the basis of our *ab initio* calculations, we introduce a low-energy effective Hamiltonian, which describes the band structure of our system, and determine its parameters. The density of states is found for these parameters.

Our main aim is to calculate the electron dispersion of low-energy excitations in a perfect planar array of zigzag quasimetallic carbon nanotubes. The tubes are assumed to be separated by the constant distance d between the walls of the tubes (see Fig. 1). In other words, the array is generated by creating a succession of exact copies of a carbon nanotube with separation along a direction normal to the tube axis. We have found the optimal distance between tubes using the Perdew-Burke-Ernzerhof (PBE)-D2 approach (see Appendix A). Our analysis includes calculation of the band structure of an isolated ($15, 0$) zigzag nanotube and an array of ($15, 0$) nanotubes separated by the optimal distance.

II. BAND STRUCTURE OF AN ISOLATED ($15, 0$) CARBON NANOTUBE

The low-energy part of the band structure of a single ($15, 0$) zigzag nanotube is shown in Fig. 2. We have checked that our results are consistent with the well-known *ab initio*

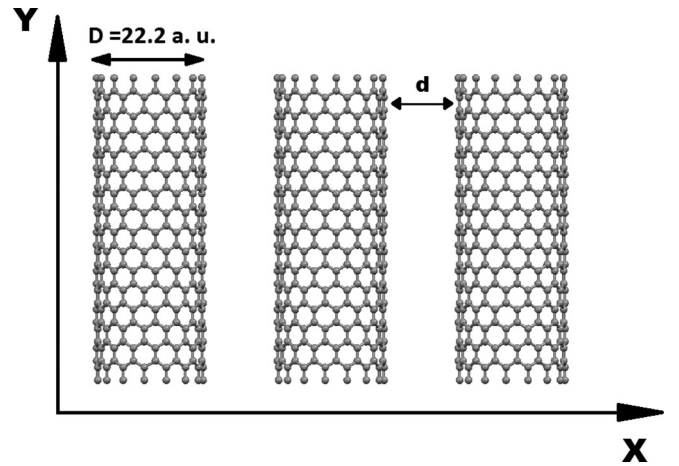


FIG. 1. A horizontally aligned array of ($15, 0$) carbon nanotubes separated by a distance d . The diameter of a ($15, 0$) CNT is 22.2 a.u. (1 a.u. = 0.529 Å).

calculations of Ref. [4], which in turn are in good agreement with the experimental data of Lieber *et al.* [25] and confirm the $E_g \propto 1/D^3$ dependence for quasimetallic CNTs with curvature-induced band gaps [22].

As expected, all the energy levels are twofold degenerate (or fourfold degenerate when the Kramers degeneracy is taken into account). For single-tube calculations, we used the QUANTUM ESPRESSO code for a three-dimensional system with widely separated nanotubes and confirmed that the dispersion in any direction normal to the nanotube axis was flat.

III. OPTIMIZATION OF THE NANOTUBE ARRAY GEOMETRY

Before calculating the optimal distance between nanotubes, we performed the convergence test leading to the use of the $10 \times 10 \times 1$ Monkhorst-Pack grid (see Appendix A).

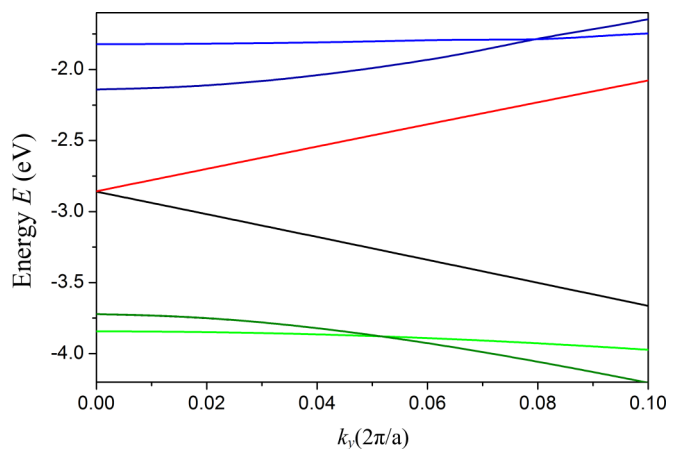


FIG. 2. The electron dispersion in a ($15, 0$) carbon nanotube along the tube axis for a small part of the Brillouin zone. The wave vector k_y is given in the reciprocal-space units. Here, a is the translation vector, which is equal to 8 a.u. All the bands are twofold degenerate. There is a small (few meV) curvature-induced band gap at $k_y = 0$.

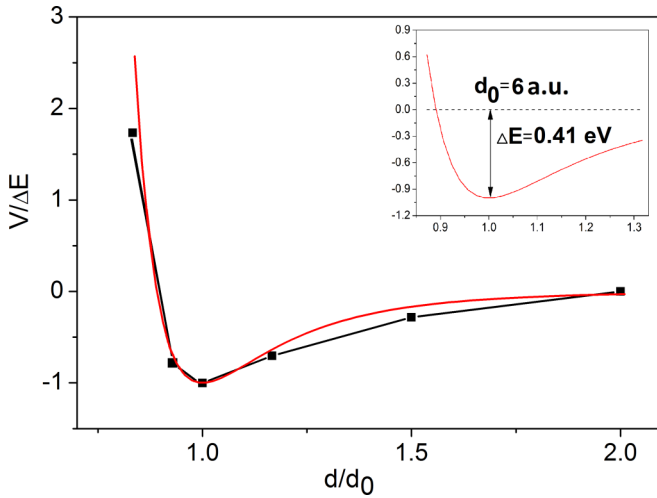


FIG. 3. The dependence of the CNT array supercell total energy V in units of the Lennard-Jones potential well depth ΔE on the normalized distance between the nanotube walls. A kinky dependence (shown in black) is the result of the PBE-D2 calculations; a smooth (red) curve represents the Lennard-Jones potential. The parameters of the best-fit Lennard-Jones potential are shown in the inset. Here, ΔE is the depth of the potential well, and $d = d_0 = 6$ a.u. corresponds to the potential minimum.

Then the PBE-D2 approach, which includes van der Waals interactions, was used to calculate the total energy of the supercell for different values of the in-plane intertube separation d .

As can be seen from Fig. 3, the total-energy dependence is well described by the Lennard-Jones potential,

$$V(d) = \Delta E \left[-2 \left(\frac{d_0}{d} \right)^6 + \left(\frac{d_0}{d} \right)^{12} \right], \quad (1)$$

where ΔE is the depth of the Lennard-Jones potential well, and $d = d_0$ corresponds to the well minimum.

By fitting the results of our *ab initio* simulations with the potential given by Eq. (3), we find that the optimal intertube

distance for the considered planar array of (15, 0) CNTs is given by $d = d_0 = 6$ a.u.

IV. NANOTUBE ARRAY ENERGY SPECTRUM

We now proceed to the results of the *ab initio* calculations of the energy spectrum of the planar array of (15, 0) CNTs separated by $d = 6$ a.u. corresponding to the optimal intertube distance governed by the van der Waals interaction. The calculated dispersions along the nanotube axis (Y axis) and in the direction normal to the nanotube axis (X axis) are shown in Figs. 4(a) and 4(b), respectively.

The striking feature of the calculated dispersion of the optimally spaced CNT array is a significant gap (around 0.12 eV) opening in the Γ point, in contrast to a tiny curvature-induced gap accompanied by a quasilinear dispersion in the Y direction and a totally flat dispersion in the X direction in the limit of large intertube separation. The band gap shrinks towards the middle of the Brillouin zone in the X direction. The dispersion along the X axis resembles the well-known single-chain tight-binding cosine spectrum with the period $b = D + d$, reflected in the horizontal axis due to electron-hole symmetry.

An important feature of this spectrum is the lifting of the twofold energy-level degeneracy existing in a single zigzag CNT due to equivalent contributions from the two graphene K points. The most drastic consequence of lifting the valley-related degeneracy in quasimetallic zigzag CNTs, when they are combined into a regular array, is the collapse of the band gap in the formed two-dimensional (2D) material. As can be clearly seen from Fig. 4(b), the two small gaps corresponding to the two formerly degenerate states of a single nanotube occur in the array at slightly different energies, which leads to an overlap of the conduction and valence bands. This unexpected dielectric-metal transition induced by the change in the system dimensionality seems to be a generic feature for closely packed arrays of $(3p, 0)$ CNTs. The results of similar calculations for the planar arrays of optimally spaced (12, 0) and (18, 0) nanotubes are presented in Appendix B. The band gaps are closed in these structures as well. Another notable feature of the zigzag nanotube array dispersion is the intersections of the lowest unoccupied molecular orbital LUMO1

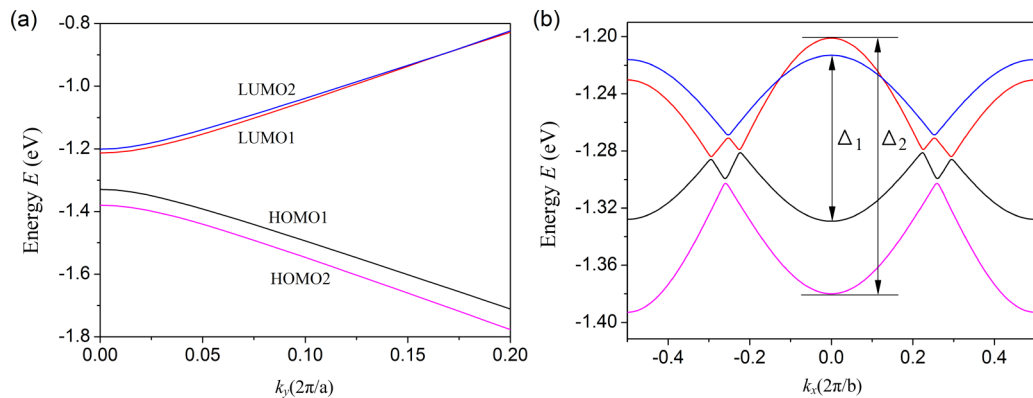


FIG. 4. The electronic band structure of an array of (15, 0) carbon nanotubes separated by $d = 6$ a.u.: (a) along the tube axis for $k_x = 0$ and (b) in the direction normal to the tube axis for $k_y = 0$. Here, Δ_1 is the band gap between the lowest unoccupied molecular orbital LUMO1 and highest occupied molecular orbital HOMO1 bands in the Γ point; Δ_2 corresponds to the LUMO2 and HOMO2 bands. The wave vectors k_y and k_x are given in reciprocal-space units. The lattice period in the X direction $b = D + d = 28.2$ a.u.

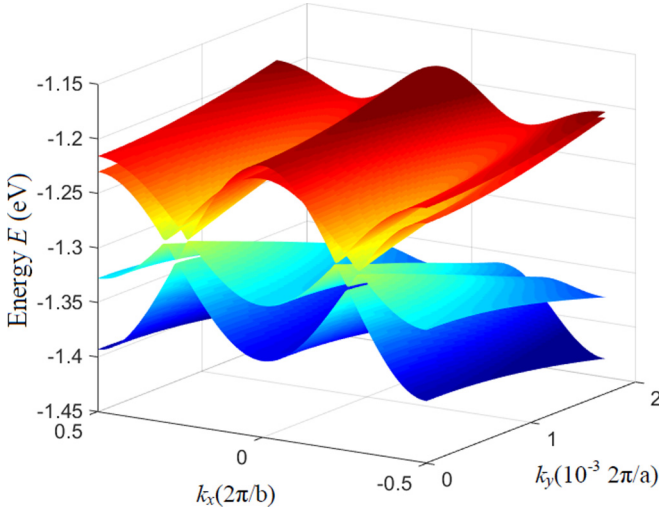


FIG. 5. The surface plot of the energy dispersion of an array of (15, 0) carbon nanotubes separated by $d = 6$ a.u. obtained within the PBE-D2 approach.

and LUMO2 bands, which can be clearly seen in Fig. 4(b) near $k_x \approx \pm 0.125$ in units of $2\pi/b$. These intersections result in the appearance of two strongly tilted Dirac cones (or Dirac grooves), which annihilate when the separation between nanotubes tends to infinity and the degeneracy between the two bands is restored. In the literature, this type of energy-band intersection is usually called type-II Dirac-Weyl point or tilted Dirac-Weyl cone with an open, hyperbolic isofrequency contour; see, e.g., [26]. In 2D systems, this type of dispersion leads to a plethora of interesting magnetotransport phenomena [27,28]. It has been discussed in relation to either functionalized graphenelike materials and strained graphene [29] or artificial hexagonal lattices [26,30], but here we associate it with carbon nanotube arrays. The discussed intersections are the consequence of the loss of the mirror symmetry, when the (3p,0) CNTs with odd p are placed in an array.

The two-dimensional surface plot of the four subbands closest to the Fermi level for the planar array of optimally separated (15, 0) CNTs is shown in Fig. 5. It clearly depicts the strong anisotropy of our system with different signs of quasiparticle effective masses in two orthogonal directions.

The main band structure parameters of the (15, 0) CNT array are summarized in Table I.

TABLE I. Band-structure parameters of the optimally spaced (15,0) CNT array. Indexes H1, H2, L1, and L2 correspond to HOMO1, HOMO2, LUMO1, and LUMO2 bands. The effective masses along x and y axes $m_{x,y}$ counted in the units of free electron mass are presented for the Γ point. Fermi velocities along the same axes $V_{fx,fy}$ are presented for the Dirac points of the two dimensional dispersion.

$V_{fx}, \frac{m}{s}$	m_x^{H2}, m_e	m_x^{H1}, m_e	m_x^{L1}, m_e	m_x^{L2}, m_e	Δ_1 (eV)
1.35×10^5	0.4	0.52	-0.56	-0.32	0.12
$V_{fy}, \frac{m}{s}$	m_y^{H2}, m_e	m_y^{H1}, m_e	m_y^{L1}, m_e	m_y^{L2}, m_e	Δ_2 (eV)
10.3×10^5	-0.068	-0.071	0.07	0.072	0.18

For comparison, we present in Fig. 6 the results of the *ab initio* energy-spectrum calculations for an optimally spaced array of armchair (9, 9) nanotubes, which have a diameter of $D \approx 23.07$ a.u. that is very close to that of the (15, 0) CNTs considered above. Notably, the optimal separation between the (9, 9) armchair CNTs, $d = 6$ a.u., is the same as between (15, 0) nanotubes in their optimally spaced array. The main consequence of combining metallic armchair nanotubes into a closely packed regular planar array is the opening of a significant band gap, so that the resulting 2D crystal becomes a dielectric (narrow-gap semiconductor). In fact, this effect is equivalent to piercing an armchair nanotube by a strong magnetic field along the CNT axis [31]. Our calculations show that the band gap in an optimally spaced (9, 9) tube is $E_g = 40$ meV, which corresponds to an effective magnetic field of 65 T. This gap opening should be accompanied by strong interband dipole transitions in the narrow range of photon energies near the band gap [17,31,32]. The dispersion remains strongly anisotropic with a very heavy effective mass in the X direction near the conduction-band minimum, and displays hyperbolic behavior near $k_y = 2\pi/3$ and either $k_x = 0$ or $k_x = \pi/b$. However, the overall low-energy band structure for an array of armchair CNTs is significantly less complex than in the case of narrow-gap zigzag nanotubes.

It should be noticed that the opening of a band gap in armchair nanotubes assembled into dense 3D bundles has been discussed in the literature [22,33,34]. However, as shown in Ref. [22], this band-gap opening depends on the system geometry and does not occur in highly symmetric hexagonal packing of tubes, so it is worth checking what happens in the 2D configuration.

V. THE MODEL HAMILTONIAN

With the insight from our *ab initio* calculations, we have constructed an approximate four-band model Hamiltonian for an array of optimally spaced gapless zigzag carbon nanotubes. The energy spectrum of the array has four Dirac cones at $k_y = 0$ and the values of k_x given by $k_x = \pm k_1$ and $k_x = \pm k_2$. Around these points, the dispersion is anisotropic such that the ratio of the Fermi velocities along the Y and X directions is $v_{Fy}/v_{Fx} \equiv \xi \neq 1$. It is also evident that the energy spectrum is split at the γ point ($\mathbf{k} = 0$). To model these characteristics, we propose the following effective Hamiltonian:

$$H = \begin{pmatrix} H_I & V \\ V & H_{II} \end{pmatrix}, \quad (2)$$

where

$$H_I = \alpha_1 \begin{pmatrix} \epsilon_1 & K_+^1 \\ K_+^1 & \epsilon_1 \end{pmatrix} + \begin{pmatrix} \beta_1 k_x^2 & 0 \\ 0 & \beta_1 k_x^2 \end{pmatrix},$$

$$H_{II} = \alpha_2 \begin{pmatrix} \epsilon_2 & K_+^2 \\ K_+^2 & \epsilon_2 \end{pmatrix} + \begin{pmatrix} \beta_2 k_x^2 & 0 \\ 0 & \beta_2 k_x^2 \end{pmatrix},$$

$$K_{\pm}^{1,2} = \left[(k_x - k_{1,2}) - \lambda_{1,2} (k_x - k_{1,2})^3 \pm \frac{ik_y}{\xi} \right]$$

$$\times \left[(k_x + k_{1,2}) - \lambda_{1,2} (k_x + k_{1,2})^3 \pm \frac{ik_y}{\xi} \right],$$

$$V = \begin{pmatrix} v & 0 \\ 0 & v \end{pmatrix}.$$

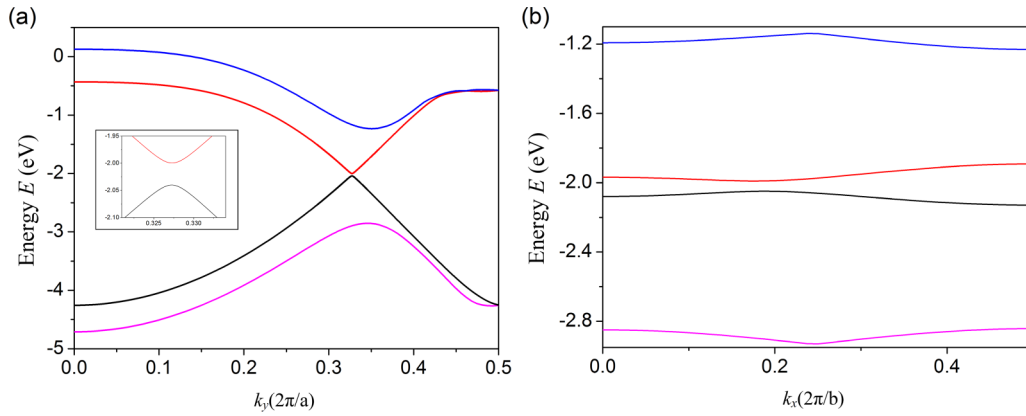


FIG. 6. The electronic band structure of an array of (9, 9) carbon nanotubes separated by $d = 6$ a.u.: (a) along the tube axis for $k_x = 0.2$ and (b) in the direction normal to the tube axis for $k_y = 0.33$. The wave vectors k_x and k_y are given in reciprocal-space units. The lattice period in the X direction is $b = D + d = 29.07$ a.u. The inset to (a) shows the energy dispersion along the Y axis in the close vicinity of the conduction-band minimum.

Here, parameters k_1 and k_2 specify the positions of the Dirac cones. The corresponding Fermi velocities are defined by α_1 and α_2 . Parameter ξ defines the ratio of the Fermi velocities in the X and Y directions. The band splitting is taken into account using parameters ϵ_1 , ϵ_2 , and v . Parameters λ_1 and λ_2 in front of the cubic terms are responsible for the bending of bands at the edges of the Brillouin zone. The electron-hole asymmetry, which is clearly seen in our density functional theory (DFT) calculations, is described by parameters β_1 and β_2 . The Hamiltonian, given by Eq. (2), approximates the low-energy part of the energy spectrum with a good accuracy.

The calculated energy bands from the *ab initio* study of the CNT array described above are fitted by the dispersion given by the low-energy effective Hamiltonian (2). In Fig. 7, we compare the results of the *ab initio* calculations with the

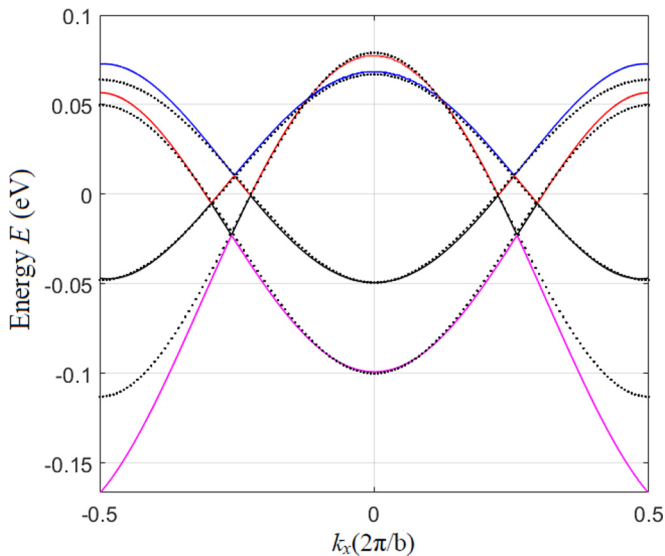


FIG. 7. The electronic band structure of the optimally spaced ($d = 6$ a.u.) array of (15, 0) zigzag nanotubes in the direction normal to the tube axis. Solid lines correspond to the band structure described by the effective Hamiltonian; dotted lines show the results of the *ab initio* calculations. Parameters of the model Hamiltonian are chosen in accordance with Table II.

proposed few-parameter approximation. The relevant parameters for the effective Hamiltonian are given in Table II. Polynomials of the order of higher than three should be taken into account in the Hamiltonian to get a more accurate dispersion.

VI. THE DENSITY OF STATES

The band structure of the considered CNT array obtained with the help of the DFT approach has four saddle points. A simple hyperbolic energy spectrum around a saddle point with energy E_0 has the form

$$E(k_x, k_y) = E_0 + \frac{\hbar^2 k_x^2}{2m_x} - \frac{\hbar^2 k_y^2}{2m_y}, \quad (3)$$

where m_x and m_y are the effective masses along the X and Y directions, respectively, which are defined as positive quantities. The effective masses are proportional to the inverse of the second derivative along the respective directions and for our system are presented in the Table I.

A calculation of the density of states (DOS) near a saddle point is outlined in Appendix C. The result is that the DOS diverges in the limit $E \rightarrow E_0$ as $\frac{1}{2} \ln[1/(E - E_0)]$. These divergences give rise to peaks known as van Hove singularities [35], which manifest themselves in peaks in the optical absorption of the system. The density of states of an array of (15, 0) CNTs separated by $d = 6$ a.u., calculated from the spectrum given by the effective Hamiltonian (2), is shown in Fig. 8. The peaks in this figure correspond to saddle points of the energy spectrum, as can be seen by comparing Figs. 7 and 8.

VII. CONCLUSIONS

We have used *ab initio* calculations to find the optimal (corresponding to the lowest total energy) geometry of a planar array of carbon nanotubes and to investigate the electron energy spectrum in the resulting superstructure. Detailed results are presented for an array of (15, 0) CNTs only; however, our further study shows that the main features of the spectrum, such as the closing of the total band gap, the appearance of tilted Dirac cones, strong anisotropy, and

TABLE II. Parameters of the effective Hamiltonian fitted to *ab initio* calculated electronic band structure for an array of optimally spaced (15, 0) CNTs. The splitting constant ν is equal to 10^{-6} a.u. The atomic system of units is used throughout the table: $\hbar = |e| = m_e = 1$.

α_1	$k_1, \frac{2\pi}{c}$	ϵ_1 (a.u.)	λ_1 (a.u. $^{-1}$)	β_1	α_2	$k_2, \frac{2\pi}{c}$	ϵ_2 (a.u.)	λ_2 (a.u. $^{-1}$)	β_2
0.039	0.255	0.00035	1.18	0.0005	0.055	0.26	-0.0004	0.98	-0.0065

the areas of negative dispersion near the Fermi level, are common for similar systems containing quasimetallic zigzag nanotubes with a different diameter. These features are caused by lifting the valley-related degeneracy when zigzag CNTs are combined in a regular planar array. In contrast, combining metallic armchair nanotubes into an optimally spaced planar array results in the opening of a significant band gap.

For an array of narrow-gap zigzag CNTs, we propose a semianalytic 4×4 Hamiltonian describing the low-energy part of the energy spectrum with its distinctive hyperbolic dispersion. The energy scale of the predicted hyperbolic dispersion makes the considered system a promising candidate for prospective applications in far-infrared optoelectronics. Indeed, the regions of negative effective mass in the low-energy part of the spectrum should lead to the appearance of negative differential conductivity, which can be used for the generation of stimulated far-infrared radiation [36,37]. The efficiency of infrared emission should be further enhanced by the presence of van Hove singularities in the relevant spectral region, which can be clearly seen from our DOS calculations. The considered structures can also be regarded as metasurfaces for electromagnetic waves in the optical to mid-infrared frequency range, which have been a subject of considerable recent research efforts [38,39].

The electronic properties of the considered system can be tuned by subjecting it to a strong magnetic field. Magnetic field behavior should reflect the system's extreme anisotropy. The component of the magnetic field normal to the array

plane will result in nontrivial Landau quantization for hyperbolic materials. The influence of the in-plane component is envisaged to be mostly via the tuning of the nanotube band gap [31,40]. Therefore, a strong dependence of the electron spectrum on the magnetic field direction should be expected.

We hope that our predictions of hyperbolic dispersion, tilted Dirac cones, and geometry-induced metal-dielectric transitions in a planar array of optimally spaced carbon nanotubes will attract significant interest from material scientists to this fascinating 2D van der Waals material. Clearly, it is a very promising system for both new exciting physics and future applications.

ACKNOWLEDGMENTS

We acknowledge support from Horizon 2020 Marie Skłodowska-Curie RISE projects CoExAN (Grant No. 644076), DiSeTCom (Grant No. 823728) and TERASSE (Grant No. 823878), Russian Mega-Grant No. 14.Y26.31.0015 and Project No. 3.2614.2017/4.6 of the Ministry of Education and Science of Russian Federation. This work was also financially supported by the Government of Russian Federation (Grant No. 08-08) including the support for M.E.P. through the ITMO Fellowship and Professorship Program. We are grateful to S. P. Hepplestone, T. P. Collier, and E. Mariani for valuable comments. P.K. is supported by Horizon 2020 IF TURANDOT project 836816 and Academy of Finland Flagship Programme, Photonics Research and Innovation (PREIN), decision 320166.

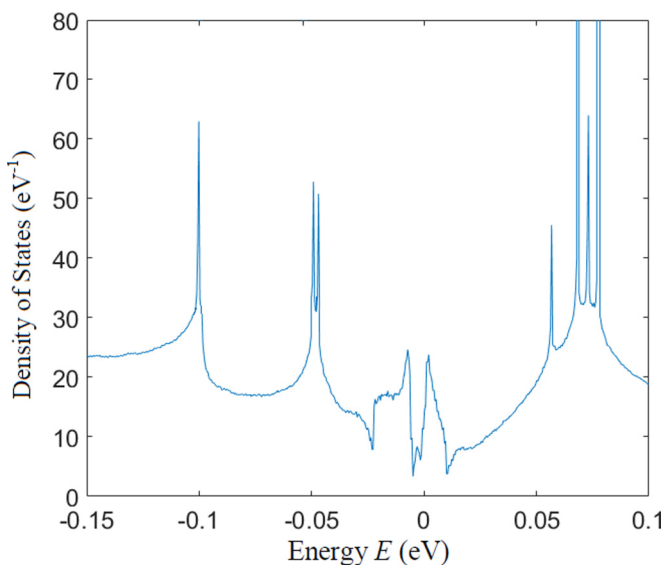


FIG. 8. The density of states of an array of optimally spaced (15, 0) carbon nanotubes calculated using the effective Hamiltonian given by Eq. (2). The sharp peaks correspond to van Hove singularities.

APPENDIX A: METHODS

The *ab initio* calculations of the band structure of the CNT array were performed with an ultrasoft pseudopotential and a plane-wave basis in the QUANTUM ESPRESSO (QE) package [41]. The QE package is based on first-principles density functional theory (DFT) [42,43]. The DFT method is a powerful tool for performing many-body electronic structure calculations. It finds a good approximate solution to the quantum mechanical many-body problem.

At the first stage, we considered a single (15, 0) zigzag carbon nanotube, which is metallic within the graphene zone-folding approximation. We examined the electronic bands of the nanotube along its axis. For the case of a (15, 0) CNT, the unit cell contains 60 atoms. To employ the QE code, a simulated nanotube was placed in a hexagonal supercell with a lattice constant of 60 a.u. A diameter of an (m, n) single-walled carbon nanotube is computed in a.u. from the expression [7] $D = 1.48\sqrt{m^2 + n^2 + mn}$, where n and m are the integer components of the chiral vector. For a (15, 0) CNT, the diameter is equal to 22.2 a.u. The exchange-correlation energy functional of Perdew, Burke, and Ernzerhof (PBE) [44] was used. The $1 \times 4 \times 1$ Monkhorst-Pack grid in k space

was used for self-consistent calculations of the electronic structure.

At the second stage, we made a convergence test with respect to the number of k points in the $n \times n \times 1$ Monkhorst-Pack grid for an infinite array of (15, 0) CNTs and different distances between tubes, varying n from 4 to 12. We used the generalized gradient approximation [45] with PBE and added the van der Waals (vdW) corrections to find the optimal distance between tubes. The vdW interaction, which governs the optimal distance between CNTs, was included by the use of the method of Grimme (PBE-D2) [46]. In order to get accurate results, the plane-wave cutoff was set to a high value of 80 Ry, for which the structural relaxations and the electronic energies are fully converged. A Gaussian smearing for the occupations was used with a width of 0.01 eV.

At the third stage, we calculated the band structure of the array of (15, 0) zigzag CNTs separated by the optimal distance d found in the second stage. The nanotube array is assumed to lie in the XY plane, and the tubes are aligned along the Y axis (see Fig. 1), so that the system is two dimensional in nature. To adapt our system to the standard QE package, we assume the CNTs to be arranged into the three-dimensional lattice with the large separation of 60 a.u. between the layers in the Z direction, so that the interaction between the tubes in this direction can be neglected. The band-structure calculations were performed within the above-mentioned DFT (PBE-D2) method.

APPENDIX B: ENERGY SPECTRA FOR OPTIMALLY SPACED ARRAYS OF (12,0) AND (18,0) CARBON NANOTUBES

In this section we provide some results of our *ab initio* calculations supporting the statement in the main text that the collapse of the band gap is a generic feature of closely packed arrays of $(3p, 0)$ zigzag carbon nanotubes.

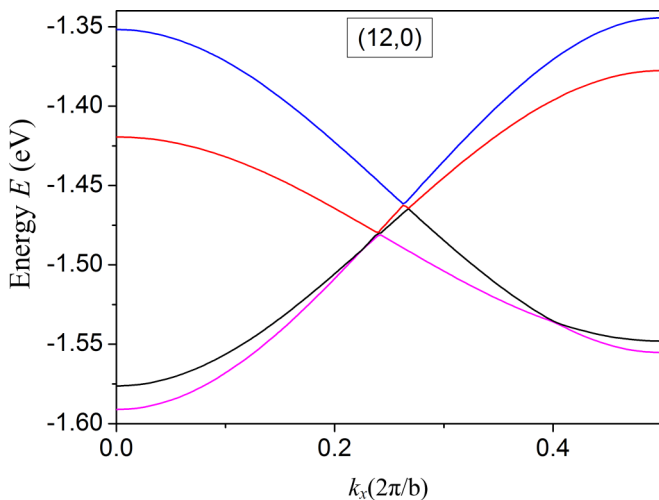


FIG. 9. The electronic dispersion of an array of (12, 0) carbon nanotubes separated by $d = 6.2$ a.u. in the direction normal to the tube axis for $k_y = 0$. The lattice period in the X direction $b = D + d = 23.96$ a.u.

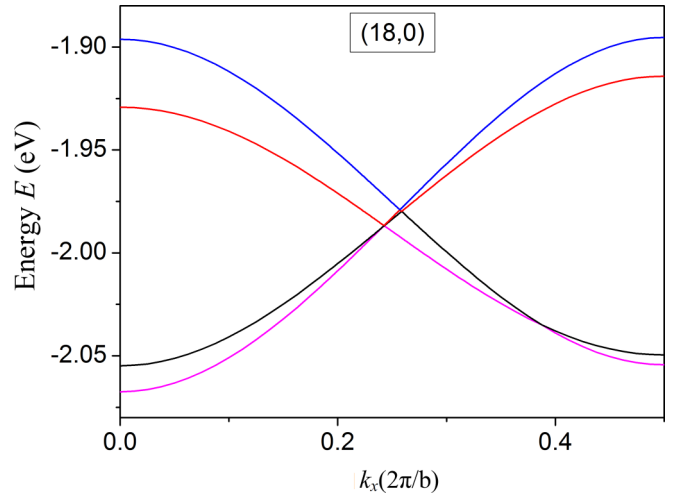


FIG. 10. The electronic dispersion of an array of (18, 0) carbon nanotubes separated by $d = 6.2$ a.u. in the direction normal to the tube axis for $k_y = 0$. The lattice period in the X direction, $b = D + d = 32.84$ a.u.

Whereas the main text is focused on (15, 0) CNTs, here we present the data for two other quasimetallic zigzag CNTs, which have either a smaller or a larger diameter than the (15, 0) CNT. Namely, here we present the data for optimally spaced arrays of (12, 0) and (18, 0) CNTs. The calculations are performed within the PBE-D2 approach described in the previous section.

In Fig. 9, we present the electronic dispersion $E(k_x)$ in the planar array of (12, 0) CNTs along the direction normal to the nanotube axis for $k_y = 0$.

A similar plot for optimally spaced planar array of (18, 0) CNTs is shown in Fig. 10. Interestingly, the optimal nanotube separation d in this array is the same as for (12, 0) CNTs, which slightly exceeds the value for (15, 0) nanotubes.

Clearly, in both cases, there is no value of energy in the low-energy part of the spectrum for which the valence band and conduction band of the zigzag-nanotube-based 2D crystal do not overlap. This indicates a metallic behavior of an array made of nanotubes which individually have curvature-induced band gaps of a few meV.

APPENDIX C: DENSITY OF STATES IN A HYPERBOLIC MATERIAL

Here, we calculate the density of states, $g(E)$, near a general saddle point, where the energy zero level is chosen to coincide with the saddle point E_0 . The energy is then given by

$$E(k_x, k_y) = \frac{\hbar^2 k_x^2}{2m_x} - \frac{\hbar^2 k_y^2}{2m_y}, \quad (C1)$$

where the positive constants m_x and m_y are the effective masses along the X and Y directions, respectively.

By definition, the density of states is given by

$$g(E) = \frac{2}{(2\pi)^2} \int_{E(\mathbf{k})=\text{const}} \frac{df_E}{|\nabla_{\mathbf{k}} E(\mathbf{k})|}, \quad (C2)$$

where df_E is a line element along the constant-energy curve [47,48], which we now proceed to find. Dividing both sides of Eq. (C1) by E , we arrive at

$$\frac{k_x^2}{a^2} - \frac{k_y^2}{b^2} = 1, \quad (\text{C3})$$

which defines a hyperbola with

$$a = \frac{\sqrt{2m_x E}}{\hbar}, \quad b = \frac{\sqrt{2m_y E}}{\hbar}.$$

The constant-energy curves are thus two hyperbolas. The parametric representation of a wave vector $\mathbf{k} = [k_x, k_y]^T$ along a hyperbola is given by

$$\begin{aligned} k_x(t) &= a \cosh t, \\ k_y(t) &= b \sinh t, \end{aligned}$$

where $t \in [-t_0, t_0]$, with the cutoff parameter t_0 defined by the condition

$$t_0 = \min \left\{ \ln \left(\frac{k_{0x}}{a} - \sqrt{\frac{k_{0x}^2}{a^2} - 1} \right), \ln \left(\frac{k_{0y}}{b} - \sqrt{\frac{k_{0y}^2}{b^2} - 1} \right) \right\}. \quad (\text{C4})$$

Now, using the standard technique for evaluating a line integral, we calculate

$$\begin{aligned} g(E) &= \frac{1}{2\pi^2} \int_{-t_0}^{t_0} \frac{|\dot{\mathbf{k}}(t)|}{|\nabla_{\mathbf{k}} E(\mathbf{k}(t))|} dt \\ &= \frac{1}{2\pi^2} \int_{-t_0}^{t_0} \frac{b \sqrt{\cosh^2 t + \eta \sinh^2 t}}{\frac{\hbar^2 \sqrt{\eta} b}{m_x} \sqrt{\cosh^2 t + \eta \sinh^2 t}} dt \\ &= \frac{1}{2\pi^2} \int_{-t_0}^{t_0} \frac{m_x}{\hbar^2 \sqrt{\eta}} dt = \frac{t_0 \sqrt{m_x m_y}}{(\pi \hbar)^2}, \end{aligned} \quad (\text{C5})$$

where

$$\eta \equiv \frac{m_x}{m_y} = \frac{a^2}{b^2}. \quad (\text{C6})$$

For small E , Eq. (C4) yields

$$t_0 \approx \min \left\{ \ln \left(\frac{2\hbar k_{0x}}{\sqrt{2m_x E}} \right), \ln \left(\frac{2\hbar k_{0y}}{\sqrt{2m_y E}} \right) \right\}. \quad (\text{C7})$$

This means that t_0 and therefore $g(E)$ diverge in the limit $E \rightarrow 0$ as $\frac{1}{2} \ln(1/E)$.

-
- [1] A. K. Geim and I. V. Grigorieva, *Nature (London)* **499**, 419 (2013).
- [2] K. S. Novoselov, A. Mishchenko, A. Carvalho, and A. H. Castro Neto, *Science* **353** (2016).
- [3] S. Iijima, *Nature (London)* **354**, 56 (1991).
- [4] Y. Matsuda, J. Tahir-Kheli, and W. A. Goddard, *J. Phys. Chem. Lett.* **1**, 2946 (2010).
- [5] J.-C. Charlier, X. Blase, and S. Roche, *Rev. Mod. Phys.* **79**, 677 (2007).
- [6] R. A. Jishi, L. Venkataraman, M. S. Dresselhaus, and G. Dresselhaus, *Phys. Rev. B* **51**, 11176 (1995).
- [7] R. Saito, G. Dresselhaus, and M. Dresselhaus, *Physical Properties of Carbon Nanotubes* (Imperial College Press, London, 1998).
- [8] X. He, W. Gao, L. Xie, B. Li, Q. Zhang, S. Lei, J. M. Robinson, E. H. Házroz, S. K. Doorn, W. Wang, R. Vajtai, P. M. Ajayan, W. W. Adams, and R. H. Hauge, *Nat. Nanotechnol.* **11**, 633 (2016).
- [9] R. Zhang, Y. Zhang, and F. Wei, *Chem. Soc. Rev.* **46**, 3661 (2017).
- [10] Y. Ichinose, A. Yoshida, K. Horiuchi, K. Fukuhara, N. Komatsu, W. Gao, Y. Yomogida, M. Matsubara, T. Yamamoto, J. Kono, and K. Yanagi, *Nano Lett.* **19**, 7370 (2019).
- [11] M. E. Green, D. A. Bas, H.-Y. Yao, J. J. Gengler, R. J. Headrick, T. C. Back, A. M. Urbas, M. Pasquali, J. Kono, and T.-H. Her, *Nano Lett.* **19**, 158 (2019).
- [12] W. Gao and J. Kono, *R. Soc. Open Sci.* **6**, 181605 (2019).
- [13] L. Ren, C. L. Pint, L. G. Booshehri, W. D. Rice, X. Wang, D. J. Hilton, K. Takeya, I. Kawayama, M. Tonouchi, R. H. Hauge, and J. Kono, *Nano Lett.* **9**, 2610 (2009).
- [14] L. Ren, C. L. Pint, T. Arikawa, K. Takeya, I. Kawayama, M. Tonouchi, R. H. Hauge, and J. Kono, *Nano Lett.* **12**, 787 (2012).
- [15] R. R. Hartmann, J. Kono, and M. E. Portnoi, *Nanotechnology* **25**, 322001 (2014).
- [16] L. V. Titova, C. L. Pint, Q. Zhang, R. H. Hauge, J. Kono, and F. A. Hegmann, *Nano Lett.* **15**, 3267 (2015).
- [17] R. R. Hartmann, V. A. Saroka, and M. E. Portnoi, *J. Appl. Phys.* **125**, 151607 (2019).
- [18] K. Yanagi, R. Okada, Y. Ichinose, Y. Yomogida, F. Katsutani, W. Gao, and J. Kono, *Nat. Commun.* **9**, 1121 (2018).
- [19] V. A. Shahnazaryan, V. A. Saroka, I. A. Shelykh, W. L. Barnes, and M. E. Portnoi, *ACS Photon.* **6**, 904 (2019).
- [20] W. Gao, X. Li, M. Bamba, and J. Kono, *Nat. Photon.* **12**, 362 (2018).
- [21] C. L. Kane and E. J. Mele, *Phys. Rev. Lett.* **78**, 1932 (1997).
- [22] S. Reich, C. Thomsen, and P. Ordejón, *Phys. Rev. B* **65**, 155411 (2002).
- [23] Y. Umeno, T. Kitamura, and A. Kushima, *Comput. Mater. Sci.* **31**, 33 (2004).
- [24] A. Osadchy, I. V. Vorobyev, D. Rybkovskiy, and E. Obraztsova, *J. Nanoelectron. Optoelectron.* **8**, 91 (2013).
- [25] M. Ouyang, J.-L. Huang, C. L. Cheung, and C. M. Lieber, *Science* **292**, 702 (2001).
- [26] C.-R. Mann, T. J. Sturges, G. Weick, W. L. Barnes, and E. Mariani, *Nat. Commun.* **9**, 2194 (2018).
- [27] M. O. Goerbig, J.-N. Fuchs, G. Montambaux, and F. Piéchon, *Phys. Rev. B* **78**, 045415 (2008).
- [28] T. Cheng, H. Lang, Z. Li, Z. Liu, and Z. Liu, *Phys. Chem. Chem. Phys.* **19**, 23942 (2017).
- [29] B. Amorim, A. Cortijo, F. de Juan, A. Grushin, F. Guinea, F. Gutiérrez-Rubio, H. H. Ochoa, V. Parente, R. R. Rolán, P. San-Jose, J. Schiefele, M. Sturla, and M. Vozmediano, *Phys. Rep.* **617**, 1 (2016).

- [30] M. Polini, F. Guinea, M. Lewenstein, H. C. Manoharan, and V. Pellegrini, *Nat. Nanotechnol.* **8**, 625 (2013).
- [31] M. E. Portnoi, M. Rosenau Da Costa, O. V. Kibis, and I. A. Shelykh, *Int. J. Mod. Phys. B* **23**, 2846 (2009).
- [32] M. E. Portnoi, O. V. Kibis, and M. Rosenau da Costa, *Superlattices Microstruct.* **43**, 399 (2008).
- [33] P. Delaney, H. J. Choi, J. Ihm, S. G. Louie, and M. L. Cohen, *Phys. Rev. B* **60**, 7899 (1999).
- [34] Y.-K. Kwon, S. Saito, and D. Tománek, *Phys. Rev. B* **58**, R13314 (1998).
- [35] L. Van Hove, *Phys. Rev.* **89**, 1189 (1953).
- [36] V. N. Bondar, A. T. Dalakyan, L. E. Vorob'ev, D. A. Firsov, and V. N. Tulupenko, *JETP Lett.* **70**, 265 (1999).
- [37] L. E. Vorob'ev, S. N. Danilov, V. N. Tulupenko, and D. A. Firsov, *JETP Lett.* **73**, 219 (2001).
- [38] A. V. Kildishev, A. Boltasseva, and V. M. Shalaev, *Science* **339**, 1232009 (2013).
- [39] I. Trushkov and I. Iorsh, *Phys. Rev. B* **92**, 045305 (2015).
- [40] G. Fedorov, A. Tselev, D. Jiménez, S. Latil, N. G. Kalugin, P. Barbara, D. Smirnov, and S. Roche, *Nano Lett.* **7**, 960 (2007).
- [41] P. Giannozzi, S. Baroni, N. Bonini, M. Calandra, R. Car, C. Cavazzoni, D. Ceresoli, G. L. Chiarotti, M. Cococcioni, I. Dabo, A. D. Corso, S. de Gironcoli, S. Fabris, G. Fratesi, R. Gebauer, U. Gerstmann, C. Gougoussis, A. Kokalj, M. Lazzeri, L. Martin-Samos, N. Marzari, F. Mauri, R. Mazzarello, S. Paolini, A. Pasquarello, L. Paulatto, C. Sbraccia, S. Scandolo, G. Sclauzero, A. P. Seitsonen, A. Smogunov, P. Umari, and R. M. Wentzcovitch, *J. Phys.: Condens. Matter* **21**, 395502 (2009).
- [42] P. Hohenberg and W. Kohn, *Phys. Rev.* **136**, B864 (1964).
- [43] W. Kohn and L. J. Sham, *Phys. Rev.* **140**, A1133 (1965).
- [44] J. P. Perdew, K. Burke, and M. Ernzerhof, *Phys. Rev. Lett.* **77**, 3865 (1996).
- [45] J. P. Perdew, J. A. Chevary, S. H. Vosko, K. A. Jackson, M. R. Pederson, D. J. Singh, and C. Fiolhais, *Phys. Rev. B* **46**, 6671 (1992).
- [46] S. Grimme, *J. Comput. Chem.* **27**, 1787 (2006).
- [47] H. Ibach and H. Lüth, *Solid-State Physics: An Introduction to Principles of Materials Science* (Springer, Berlin, 2009).
- [48] N. Ashcroft and N. Mermin, *Solid State Physics* (Saunders College, Philadelphia, 1976).